PHYSICAL REVIEW B VOLUME 12, NUMBER 8 15 OCTOBER 1975

Exchange enhancement of Co^{2+} and Mn^{2+} transitions due to radiation defects*

K. H. Lee and W. A. Sibley
Physics Department, Oklahoma State University, Stillwater, Oklahoma 74074
(Received 19 May 1975)

A study of the radiation-induced impurity optical transitions in $KMgF_3$ crystals has been made. It is found that the enhanced oscillator strength of the defect centers is predominately due to exchange. The data indicate that most of the transitions are due to perturbed Mn^{2+} and Co^{2+} transitions. Investigation of the effects of radiation temperature, optical bleaching, and annealing on the optical properties of $KMgF_3$:Mn^{2+} indicates that two types of defects are involved. One is a F-center–Mn^{2+} defect and the other is tentatively identified as an interstitial–F-center–Mn^{2+} defect.

I. INTRODUCTION

Recently, a number of studies of the effect of radiation on the optical properties of $3d$-impurity-ion doped $KMgF_3$ and MgF_2 crystals have been made.[1–3] One of the more interesting aspects of these investigations has been the observation of large oscillator-strength increases for previously forbidden transitions when radiation defects are present. Since the forbidden transitions are both spin and parity forbidden, in the particular host crystals used, the presence of nearby defects results in symmetry change and hence selection-rule change. Exchange between the radiation-damage defects and the transition-metal ion impurities can also affect the intensity of the optical transitions. The F center, a negative-ion vacancy with a trapped electron present for charge compensation, in $KMgF_3$ has a rather extended wave function, even in the ground state, compared to a flourine ion, and should lend itself to exchange interactions. An investigation of whether symmetry or exchange effects are most effective in enhancing the intensity of the optical transitions seems in order.

Fortunately, McClure,[4] Ferguson,[5] Liehr,[6] Tanabe and Sugano,[7] and numerous others[8–10] over the last decade or so have done an excellent job of building a base of knowledge of $3d$-ion transitions in unirradiated material. This information can be used to help designate the various optical transitions for Mn^{2+} and Co^{2+} in irradiated material. In principle, it should also be possible to utilize ligand field theory to determine how the wave functions and interelectron repulsion energies are affected by changes in environment. However, as Ferguson[5] points out, deeper understanding on this level must arise from more detailed theory and a greater availability of experimental data. It is the purpose of this paper to contribute to the latter need and to use, as far as possible, the available theory to gain insight into the perturbed transitions of $3d$ ions.

II. EXPERIMENTAL

The crystals used in these experiments were grown by the Stockbarger method in the crystal growth laboratory at Oklahoma State University. Impurity concentrations were measured by mass spectroscopy and were as follows: $KMgF_3$:Mn, 8000 ppm and $KMgF_3$:Co, 300 ppm. Irradiations were performed with an accelerator using 1.5-MeV electrons at a current of about 0.2 $\mu A/cm^2$ on the sample. The crystals were placed in a Cryogenerator or a standard helium cryostat for both irradiation and measurement. In the cryogenerator the temperature could be controlled to ± 1 K between 15 and 300 K. Optical absorption was measured using a Cary 14 spectrophotometer and emission was detected with a 1-m monochromator and associated electronics.[3] Excitation spectra were taken using exciting light from a Spex 22-cm monochromator chopped at 450 Hz, and polarized spectra were obtained using Glan polarizers or unsupported Polaroid ultraviolet sheets. Variation in the intensity of the exciting light with wavelength was calibrated and the excitation spectra have been corrected for this effect. Optical bleaching of the irradiated crystals was accomplished with light from a mercury lamp either through a filter transmitting light from 200 to 400 nm or unfiltered. A systematic study of the effect of radiation time or bleaching time on the optical properties was not undertaken.

III. RESULTS

The absorption spectra of electron-irradiated $KMgF_3$:Mn both before and after a mercury-light optical bleach at 15 K are portrayed in Fig. 1. Prior to irradiation no optical absorption bands were evident in this spectral region; but after irradiation the great complexity of the spectrum is obvious. In undoped $KMgF_3$ irradiated at 300 K, several bands are evident and have been previously identified. These bands are (i) the F band which

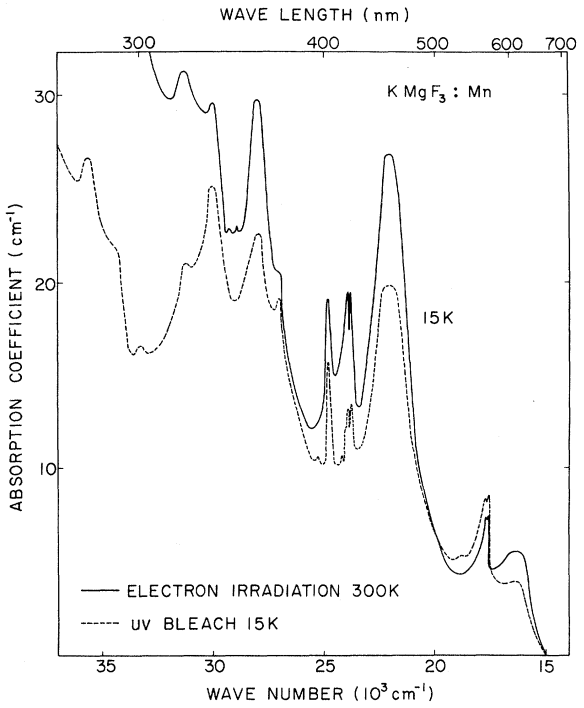

FIG. 1. Absorption spectrum from 300-K electron-irradiated $KMgF_3$: Mn crystal measured at 15 K.

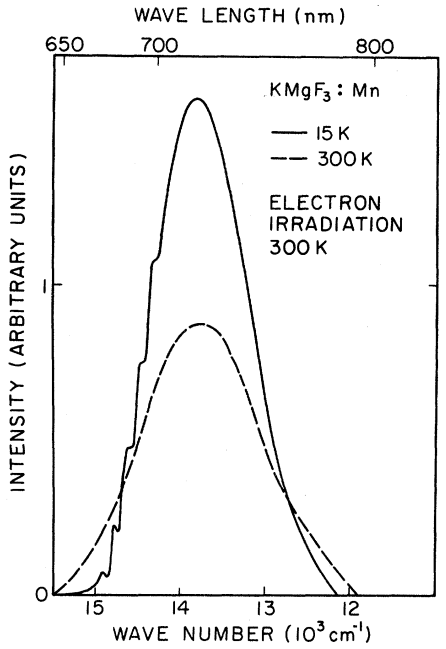

FIG. 2. 720-nm emission band from 300-K electron irradiated $KMgF_3$: Mn crystal measured at 15 K.

absorbs light of 270 nm, (ii) the F_2 or M band which absorbs at 445 nm, and (iii) a very small F_3 or R band which absorbs at 395 nm. In addition, there is a small radiation-dose-dependent band complex that appears at about 570 nm. It is evident in Fig. 1 that these bands appear in the spectrum as well as other bands which are discussed below. Optical bleaching and excitation spectra allow us to unravel the various contributors to the spectra in Fig. 1 and determine which types of defects are responsible for the various bands. Specifically, it should be noted that, although the bands at 612 nm (16 330 cm^{-1}) and 420 nm (23 800 cm^{-1}) decrease markedly with bleaching at 15 K, the bands at 563 nm (17 700 cm^{-1}) and 406 nm (24 600 cm^{-1}) retain their intensity even though the background absorption changed. However, at 300 K, it is possible to bleach the 406 and 563 nm bands with F light. The broad band at 454 nm (22 000 cm^{-1}), which is possibly due to perturbed F_2 (M) centers, is also decreased by the low-temperature bleach. The band at 563 nm (17 700 cm^{-1}) is a double peak with splitting of 63 cm^{-1}. The 420-nm (23 800 cm^{-1}) band is split by 119 cm^{-1}. The background absorption caused by the presence of a number of radiation-induced defects makes it difficult to study Mn^{2+}-radiation-defect absorption, and in the past excitation spectra have been used to obtain a clearer idea of the optical transitions of these defects.[3] The emission from what we believe is a Mn^{2+}–F-center defect[3] occurs at 720 nm (13 750 cm^{-1}) and is pictured in Fig. 2. The sharp lines on the high-energy side of the broad band are due to phonons. When a detection system is set to monitor the intensity of the 720-nm emission and exciting light of wavelength from 200 to 700 nm is allowed to strike the crystal, an excitation spectrum such as that illustrated by the full curves in Fig. 3 is obtained. These transitions, as will be discussed in more detail later, match well in relative intensity and half width with those previously observed for Mn^{2+}.[5] This leads us to believe they are associated with Mn^{2+}. However, the oscillator strengths of these transitions in irradiated specimens are several orders of magnitude greater than in unirradiated crystals.

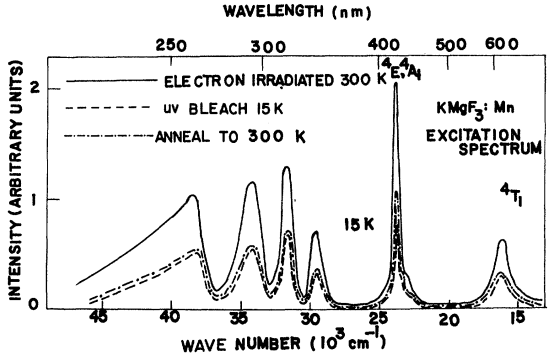

FIG. 3. Excitation spectrum for the 720-nm emission band from 300-K electron irradiated $KMgF_3$: Mn measured at 15 K.

In fact, a Mn^{2+} excitation spectrum cannot be obtained with our equipment for unirradiated samples since the intensity is too low.

As mentioned earlier, the optical transitions for Mn^{2+} in O_h symmetry are both spin and symmetry forbidden. In order to determine if the increased oscillator strength is due to site-symmetry change or to exchange interactions between the Mn^{2+} and a neighboring F center, as we have tentatively proposed in the past,[3] the following experiment was done. An irradiated sample was bleached with ultraviolet light at 15 K. This releases electrons from the F centers into other traps, but at this low temperature the empty vacancy is not mobile and the site symmetry remains almost the same as for the F-center–Mn^{2+} defect.[11] As can be seen from the data in Fig. 3, optical bleaching causes a marked decrease in the intensity of the spectrum. If site symmetry alone were responsible for the oscillator-strength changes, then this reduction would not occur. Therefore, we feel justified in indicating that exchange plays a major role in enhancing the optical transitions in this material.

In our previous work,[3] two different types of radiation-defect–Mn^{2+} complexes appeared to be present. These were tentatively identified as F-center–Mn^{2+} complexes and F-center–Mn^{2+}–interstitial complexes. The reasoning behind the assignments was based on the observation that for low-temperature irradiation one type of complex was observed, whereas for high-temperature irradiation the other complex dominated. In fact,

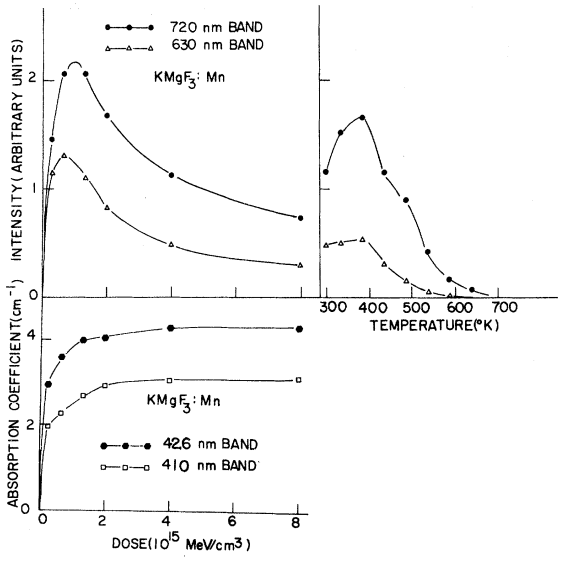

FIG. 4. Growth curves of 630-nm and 720-nm emission bands, and 426-nm (420-nm 15-K) and 410-nm (406-nm 15-K) absorption bands with radiation dose. Annealing curves of 630-nm and 720-nm bands from 300-K electron irradiated $KMgF_3$: Mn.

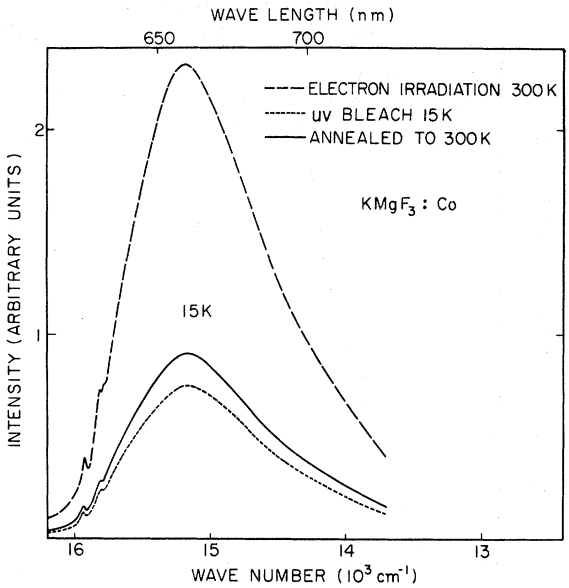

FIG. 5. 658-nm emission band from 300-K electron irradiated $KMgF_3$: Co measured at 15 K.

although it has still not been possible to detect the absorption spectrum of the so-called F-center–Mn^{2+} complex in a 15-K irradiated sample until after it has been warmed to room temperature, careful measurements on samples irradiated at 300 K disclose, as can be seen in Fig. 1, optical bands at 406 and 563 nm characteristic of the proposed F-center–Mn^{2+}–interstitial complex. At 300 K the emission bands associated with these models are located at 720 and 630 nm, respectively. For a sample irradiated at 300 K, the intensity differences between these two emission bands are shown in Fig. 4. The 720-nm emission is more intense, but both emissions have similar growth and decay characteristics. When the sample is thermally annealed above room temperature, the emission from the two bands has the characteristics also shown in Fig. 4. For 15-K irradiation the 630-nm band is more intense and the 720-nm band is extremely weak.

When $KMgF_3$: Co is irradiated, a number of new emission bands are detected. Three of these do not appear to be due to simple radiation-induced defects such as F_2 centers, but have halfwidths and vibronic structure more closely resembling that of $3d$ impurity transitions. These bands are portrayed in Figs. 5–7. As will be seen, the bands at 875 nm (11 400 cm^{-1}) and 830 nm (12 000 cm^{-1}) have the same excitation spectra, but the 658 nm (15 000 cm^{-1}) band has a quite different excitation spectrum. On the other hand, all three bands appear to grow equally with radiation, and the data illustrated in Fig. 8, which is a plot of the intensities of zero-phonon lines associated with

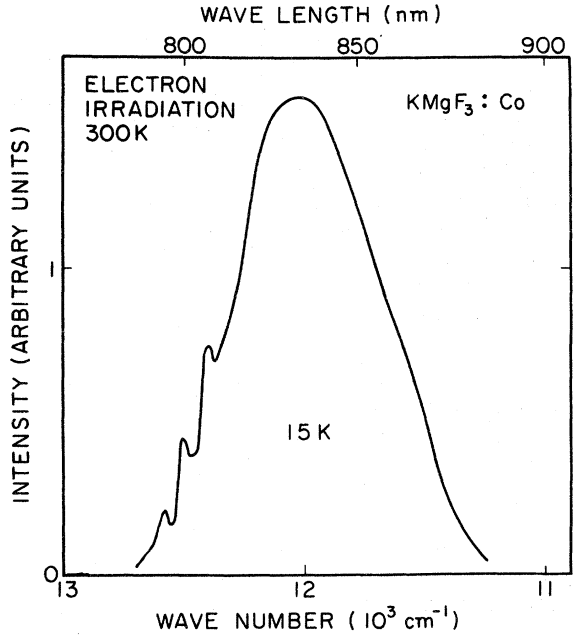

FIG. 6. 830-nm emission band from 300-K electron irradiated $KMgF_3$: Co measured at 15 K.

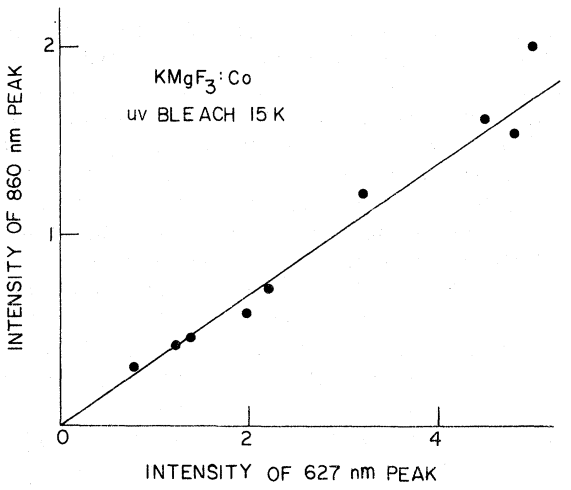

FIG. 8. Intensity relationship of zero-phonon lines of 875-nm and 658-nm emission bands as a function of radiation dose and optical bleaching.

these bands with optical bleaching, suggest that the 658 nm (15000 cm^{-1}) band and the other two come from the same defect complex. In order to determine if optical bleaching in the F-band region (280 nm) would decrease the intensity of these bands as it does for Mn^{2+}–F-center complexes, the samples were bleached at 15 K. The results are shown in Figs. 5–7 and were similar for all three bands. If the crystals were warmed to room temperature after bleaching, some recovery took place just as in the Mn^{2+} case. Since the growth of the bands with radiation appears to be the same and the effect of optical bleaching on all three is the same, we suggest that these three bands are due to a Co^{2+}–radiation-defect complex, and the increase in intensity compared with unperturbed Co^{2+} is due to exchange interactions. The excitation spectrum for the three bands is shown in Fig. 9. It should be noted that excitation at 445 nm yields an M-center emission at 585 nm, which can give problems in measuring the 658-nm excitation spectrum. This effect has been corrected for in Fig. 9.

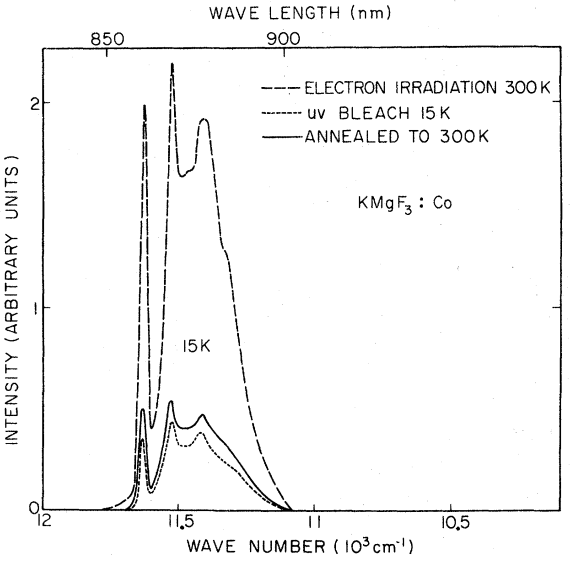

FIG. 7. 875-nm emission band from 300-K electron irradiated $KMgF_3$: Co measured at 15 K.

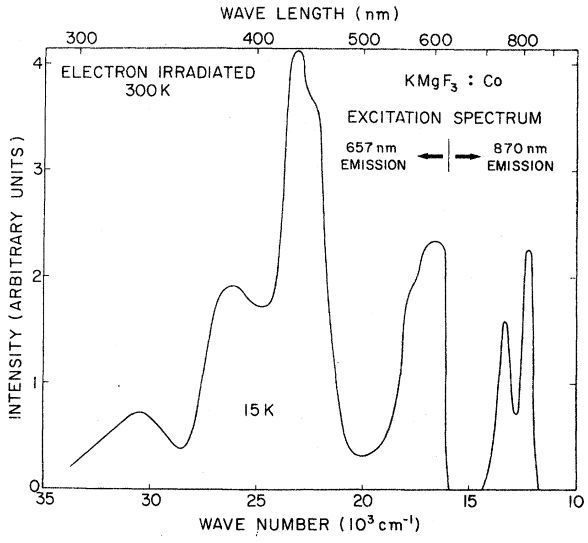

FIG. 9. Excitation spectrum for the 657-nm and 870-nm emission peaks.

IV. DISCUSSION

First, it must be illustrated that the spectra shown in Figs. 3 and 9 are actually associated with Mn^{2+} and Co^{2+} impurities. In an attempt to ascertain this, the polarized excitation spectrum from $KMgF_3$:Mn was measured. The sample was illuminated with light propagating along a [001] crystal axis, having its electric vector oriented along [100] or [010] crystallographic directions. The detected emitted light propagated along a [010] direction and the polarizers were oriented to pass the [100] or [001] electric vectors. The 720-nm emission band was used to monitor the excitation spectrum. This emission band arises from a transition between a perturbed $^4T_{1g}$ level (the presence of an F-center reduces the symmetry of a Mn^{2+} site from O_h to C_{4v} with a commensurate decomposition of the energy-level symmetry to $A_2 + E$)[12] and the $^6A_{1g}$ (in the perturbed state A_1) ground state. For electric-dipole transitions between these levels, only transitions perpendicular to the defect axis, π transitions, are allowed, while the transitions along the defect dipole axis, σ, are forbidden. This means that the 720-nm emission should be π polarized. Moreover, since the 612-nm absorption-band levels must be $A_2 + E$ symmetry, this absorption must be π polarized. The 420-nm levels are of A_1 and B_1 symmetry, and hence, the transition is σ polarized. With this in mind, a table can be constructed predicting the effects of polarized excitation and emission. We designate the intensity of the emission stimulated by [100] polarized light and measured through a [100] oriented polarizer as I_{11}. For [100] exciting light and a [001] analyzer, the intensity is I_{21}, and for [010] exciting light and a [001] analyzer the intensity is written I_{22}. In the case of unpolarized exciting light, we write I_{1u} and I_{2u} for the analyzer oriented along [100] and [001], respectively. Table I shows the predicted[13,14] and measured values for 720-nm light, as shown in Fig. 10, assuming that these transitions are from perturbed Mn^{2+} centers.

The agreement certainly suggests that these are perturbed Mn^{2+} transitions. Further evidence that the bands in Figs. 3 and 9 are due to perturbed Mn^{2+} and Co^{2+} transitions is shown in Table II. In this table we show the energies of the various levels as predicted by ligand field theory for the values of the crystal-field parameters Dq and B

TABLE I. Polarized absorption from irradiated $KMgF_3$:Mn.

	612-nm absorption			420-nm absorption		
	I_{21}/I_{11}	I_{12}/I_{22}	I_{1u}/I_{2u}	I_{21}/I_{11}	I_{12}/I_{22}	I_{1u}/I_{2u}
Predicted	0.5	1.0	1.5	∞	1.0	0.5
Observed	0.5	1.1	1.4	3.0	1.1	0.8

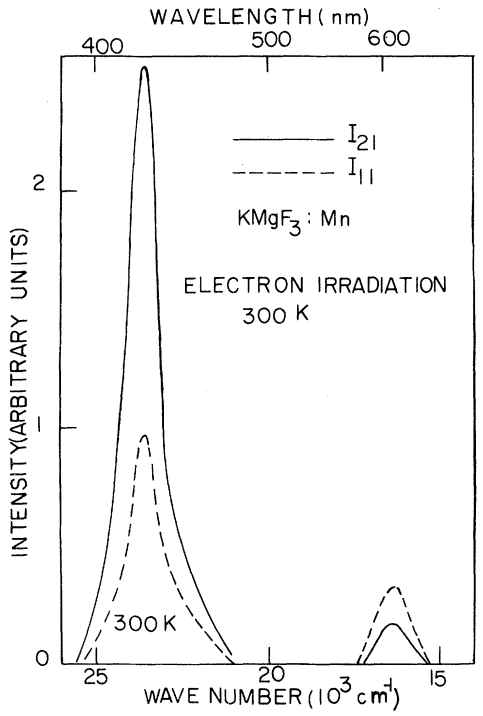

FIG. 10. Polarized excitation spectrum for polarized 720-nm emission from 300-K electron irradiated $KMgF_3$:Mn.

shown. The predictions were made using a computer program to calculate the various energies. The program diagonalizes the energy matrices given by Tanabe and Sugano.[7] For Co^{2+}, C was fixed as $4.4B$ (the same as for the free ion),[6] and the values of the Racah parameters B and Dq were then adjusted to obtain the best fit for the $^2E(^2H)$ and $^4A_2(^4F)$ levels. For Mn^{2+}, we set[15] $C = 3.453B$ and adjusted the values of B and Dq to obtain the best fit of $^4T_1(^4G)$ and $^4E(^4G)$. After this normalization procedure for the first two energy levels, no other adjustments were made. The measured and calculated values shown in parentheses are for zero-phonon-line transitions. The theory should be more applicable for zero-phonon lines, and the values of B and Dq do vary somewhat when broad band energies or zero-phonon-line energies are used. The agreement between theory and experiment for the $^4A_{2g}$ level is better when the zero-phonon energies are used, as can be seen in Table II.

The agreement between the predicted and measured absorption energies shown in Table II again suggests that the transitions are from perturbed Mn^{2+} and Co^{2+} ions. The Tanabe-Sugano diagram[7] for d^7 ions indicates that the temperature dependence of emission-band energies can be predicted. For a transition between the ^2E_g ($A_1 + B_1$ perturbed) level and the ground-state $^4T_{1g}$ level, the peak should shift to higher energy at higher tempera-

tures. This behavior is exhibited by the 875-nm emission band, as portrayed in Fig. 11, and we tentatively assign this emission to the transition between these two levels. The peak of the emission transition between the $^4A_{2g}$ (B_1 perturbed) and the $^4T_{1g}$ ground state should move, according to an analysis of the Tanabe-Sugano diagram, to lower energy at higher temperatures and be very temperature dependent. This character is evidenced by the 830-nm emission band, and we tentatively assign it to the above transition. The 658-nm band is assigned to the $^2T_{1g}$ to $^4T_{1g}$ transition of Co^{2+}. Absorption bands similar to those shown in the excitation spectrum of Fig. 9 have been found previously by Aked and Simkin[16] in γ-irradiated $KMgF_3$: Co. As can be seen from a comparison of Figs. 1 and 3 of this work, absorption spectra can be much more complex than excitation spectra and thus are more difficult to interpret. Although they

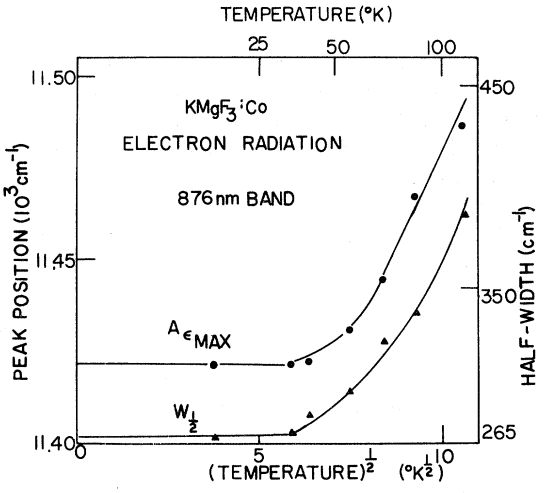

FIG. 11. Temperature dependence of half width and peak position of 875-nm emission band from 300-K electron irradiated $KMgF_3$: Co.

TABLE II. Observed and calculated spectrum for Co^{2+} and Mn^{2+} in irradiated $KMgF_3$.

Nature of defect	Energy level	Observed (10^3 cm^{-1})	Calculated (10^3 cm^{-1})
Co^{2+}–F-center	$^4T_2(^4F)$	(a) ···	6.16 (5.82)
	$^2E(^2H)$	12.19 (11.62)	12.19 (11.62)
$B = 948.8$ cm^{-1},	$^4A_2(^4F)$	13.32 (12.59)	13.32 (12.59)
$C = 4.4B$,	$^2T_1(^2H)$	16.60 (15.94)	17.59 (16.72)
$Dq = 716.4$ cm^{-1}	$^2T_2(^2H)$	17.75	17.92 (17.08)
($B = 901.9$ cm^{-1},	$^4T_1(^4F)$	···	19.39 (18.40)
$C = 4.4B$,	$^2T_1(^2G)$	22.35	22.28 (21.16)
$Dq = 667.0$ cm^{-1})	$^2A_1(^2G)$	23.10	22.48 (21.33)
	$^2T_2(^2G)$	···	25.44 (24.15)
(a) Data From Fig. 9	$^2T_1(^2F)$	26.20	26.16 (24.83)
	$^2E(^2G)$	···	28.12 (25.68)
	$^2T_1(^2P)$	30.50	31.49 (29.37)
Mn^{2+}–F-center	$^4T_1(^4G)$	(b) 16.33	16.33
	$^4T_2(^4G)$	···	20.93
$B = 873.33$ cm^{-1}	$^4A_1(^4G)$	23.81	23.81
$C = 3.453B$,	$^4E(^4G)$	23.81	23.81
$Dq = 955.2$ cm^{-1}	$^4T_2(^4D)$	···	27.64
	$^4E(^4D)$	29.60	29.92
(b) Data from Fig. 3	$^4T_1(^4P)$	31.70 34.20	33.27
	$^4A_2(^4F)$	38.50	40.30
Interstitial–Mn^{2+}–F-center	$^4T_1(^4G)$	(c) 17.70 17.76	17.76
$B = 903.44$ cm^{-1}	$^4T_2(^4G)$	20.83 22.73	22.20
$C = 3.453B$,	$^4E(^4G)$	24.03 24.63	24.63
$Dq = 897.34$ cm^{-1}	$^4A_1(^4G)$	24.75	24.63
	$^4T_2(^4D)$	28.41 29.07	28.79
(c) Data from Ref. 21	$^4E(^4D)$	30.12 30.96	30.95
	$^4T_1(^4P)$	32.57 34.13 35.70	33.87
	$^4A_2(^4F)$	38.72	41.71

interpret most of their bands as due to perturbed color centers, Aked and Simkin[16] show data that have an important bearing on our work. Their annealing data indicate that bands at about 308, 345, and 600 nm anneal out together around 500 K. Although a band around 385 nm anneals at a lower temperature, this is still a suggestion that the bands are connected to a particular defect. More important, they find an 800-nm absorption band present after irradiation with a zero-phonon transition at 860-nm, which is the same energy as the zero-phonon emission line in the 875-nm emission (Fig. 7).

Fine structure is observed on all of the bands illustrated in Figs. 5–7. This fine structure can arise from phonon-electron interactions, spin-orbit effects, or a Jahn-Teller effect. The four normal modes of vibration in $KMgF_3$ have been measured as $\nu_1 = 450$–478 cm^{-1}, $\nu_2 = 295$–300 cm^{-1}, $\nu_3 = 140$–156 cm^{-1}, and $\nu_4 = 310$–350 cm^{-1}.[17,18] Most of the Co^{2+} levels are spin-orbit split with the ground state having the largest splitting of about 1000 cm^{-1}, with the lowest two levels being about 333 cm^{-1} apart.[6,19] In fact, in MgF_2: Co where the Co^{2+} symmetry is D_{2h}, the levels are split by 152, 798, 1091, 1256, and 1398 cm^{-1} in the ground state.[20] An F-center defect next to a Co^{2+} ion reduces the symmetry and further splits the levels. The energy differences between the sharp lines in our spectra are shown in Table III. There is no marked temperature dependence of these lines relative to one another, and thus the transitions most likely originate in the lowest excited level. The splitting will then either give information on the spin-orbit splitting of the ground state or on the dominant phonon modes interacting with the

TABLE III. Spacing of sharp emission lines at 15 °K.

Emission band (nm)	Peak position nm (cm^{-1})	Energy difference (cm^{-1})	
$KMgF_3$: Co			
658	627.4 (15939)	...	
(excitation)			
590 nm	632.2 (15818)	121	121
830	794.0 (12594)	...	
(excitation)	800.5 (12492)	102	102
746 nm	806.8 (12395)	200	98
875	860.0 (11628)	...	
(excitation)	868.0 (11521)	107	107
820 nm	875.9 (11417)	211	104
$KMgF_3$: Mn			
720	670.6 (14912)	...	
(excitation)	677.8 (14754)	158	158
420 nm	684.7 (14605)	307	149
	692.0 (14451)	461	154
	699.1 (14304)	608	147

defect. An alternate method of determining the average phonon energy of the dominant interacting phonon modes is to measure the temperature dependence of the width at half maximum of absorption or emission bands and use the linear-coupling approximation. At very low temperature, the width at half maximum of the bands can be written in terms of a phonon generation term S, the so-called Huang-Rhys factor, as $W^2(0) = S(\hbar\omega)^2 8 \ln 2$, where ω is the energy of the dominant phonon modes. At a particular temperature T, the half width can be expressed as $W^2(T) = W^2(0) \coth(\hbar\omega/2kT)$. From a plot of arc coth $[W(T)/W(0)]^2$ vs $1/T$ for the 658, 830, and 875-nm bands in $KMgF_3$:Co and the 720-nm band in $KMgF_3$: Mn, we find $\nu_{658} = 139$ cm^{-1}, $\nu_{830} = 114$ cm^{-1}, $\nu_{875} = 91$ cm^{-1}, and $\nu_{720} = 223$ cm^{-1}. The values of the Huang-Rhys factor for the Co^{2+} doped crystal are $S_{658} = 9.3$, $S_{830} = 9.2$, and $S_{875} = 1.6$. It is also possible to measure S by comparing the area of the zero-phonon line to that of the broad band. This method yields $S_{658} = 5.6$, $S_{830} = 6.0$, and $S_{875} = 2.3$. The expression $P_{n0} = (S^n/n!)e^{-S}$, which arises from the linear-coupling theory, yields the ratio of the areas of the zero-phonon line and the one-phonon lines. The areas of the lines in our data are sufficiently close to those predicted that it is not possible to eliminate vibronic transitions as being responsible for the fine structure in Figs. 5–7. In fact, consideration of the data indicates that it is impossible at this time to state whether the sharp-line structure is due to electron-phonon interactions, spin-orbit splitting, the Jahn-Teller effect, or a combination of these.

In the case of irradiated $KMgF_3$:Mn, the annealing curve for the 630-nm emission band, shown in Fig. 4, has the same character as that shown for the 406- and 563-nm absorption bands in Ref. 1. Since the excitation spectrum for the 630-nm band corresponds to the absorption bands studied in Ref. 1, the data available on the 630-nm emission and on these absorption bands can be combined to yield a more accurate concept of the defect complex responsible for the emission and absorption. It is known from previous work that the 630-nm emission arises from a symmetry split level of the $^4T_{1g}$ level, and that the A_2 level of this symmetry split level is 400 cm^{-1} below the 630-nm level.[21] It can be seen in Fig. 1 that the 563-nm absorption band from which this 630-nm emission originates is split into two bands 63 cm^{-1} apart. The absorption intensity of these two bands is about the same, suggesting the transitions are allowed. We believe that this suggests the 563-nm $^4T_{1g}$ level is split into 3 levels $(B_1 + B_2 + A_2)$ in C_{2v} symmetry by the presence of the low-temperature radiation-induced defects, the $A_2 \rightarrow A_1$ transition being responsible for the 680-nm emission observed at low temperature.[21] In the first paper[1] on $KMgF_3$:Mn, with only absorption data available, we postulated that the 406- and 563-nm bands were due to F centers trapped between *two* Mn^{2+} impurity ions. The fact that the defect responsible for these bands had ⟨100⟩ symmetry and that the concentration of defects increased with impurity concentration suggested this model. In light of the present data and those in Ref. 3, we feel that two Mn^{2+} ions are probably not involved. The apparent C_{2v} symmetry of the defect can adequately be explained by a split-interstitial–Mn^{2+}–F-center complex, similar to that postulated in Ref. 3. This is a simpler model than the one involving two Mn^{2+} ions and thus far is consistent with all of our available data. In fact, Ikeya and Itoh[22] have described a split-interstitial ion-Mn^{2+} center from their EPR data on irradiated NaCl:Mn^{2+} which, if an F center were present, would be very much like the model we propose.

Perhaps the most important point of this paper is that exchange effects are responsible for the enhanced oscillator strnegths observed for $3d$-ion transitions in irradiated $KMgF_3$:Mn and $KMgF_3$:Co. Exchange effects are complicated as Anderson[23] has noted, but Ferguson *et al.*[24,25] have shown conclusively that super exchange in $KMgF_3$:Mn can increase oscillator strengths by an order of magnitude. We feel that now sufficient experimental evidence of F-center–electron-$3d$–impurity-ion exchange has been given that a theoretical investigation of wave-function overlap should be undertaken.

V. SUMMARY

Many of the absorption and emission bands observed in irradiated $KMgF_3$:Mn and $KMgF_3$:Co can

be identified as due to radiation defect–$3d$-impurity complexes. The high strength of these transitions appears to be due to exchange interactions between F centers and the $3d$ impurities.

*Work supported by NSF Grant GP-29545.

[1]W. E. Vehse and W. A. Sibley, Phys. Rev. B 6, 2443 (1972).
[2]S. I. Yun, L. A. Kappers, and W. A. Sibley, Phys. Rev. B 8, 773 (1973).
[3]S. I. Yun, K. H. Lee, W. A. Sibley, and W. E. Vehse, Phys. Rev. B 10, 1665 (1974).
[4]D. S. McClure, in *Solid State Physics*, edited by F. Seitz and D. Turnbull (Academic, New York, 1959), Vol. 9, p. 399.
[5]J. Ferguson, in *Progress in Inorganic Chemistry*, edited by S. J. Lippard (Interscience, New York, 1970), Vol. 12, p. 159.
[6]A. D. Liehr, J. Phys. Chem. 67, 1314 (1963).
[7]Y. Tanabe and S. Sugano, J. Phys. Soc. Jpn. 9, 753 (1954).
[8]J. S. Griffiths, *The Theory of Transition-Metal Ions* (Cambridge U. P., Cambridge, England, 1961).
[9]L. E. Orgel, J. Chem. Phys. 23, 1822 (1955).
[10]J. W. Stout, J. Chem. Phys. 31, 709 (1959).
[11]M. A. Young, E. E. Kohnke, and L. E. Halliburton, ESR data (private communication).
[12]F. A. Cotton, *Chemical Applications of Group Theory* (Wiley, New York, 1971).
[13]C. R. Riley, S. I. Yun, and W. A. Sibley, Phys. Rev. B 5, 3285 (1972).
[14]P. P. Feofilov, *The Physical Basis of Polarized Emission* (Consultants Bureau, New York, 1961).
[15]D. Curie, C. Barthou, and B. Canny, J. Chem. Phys. 61, 3048 (1974).
[16]N. Aked, M.S. thesis (McGill University, 1973) (unpublished); and N. H. Aked and D. J. Simkin, Bull. Am. Phys. Soc. 18, 1578 (1973).
[17]G. Hunt and C. H. Perry, Phys. Rev. 134, A688 (1964).
[18]I. Nakagawa, A. Tsuchida, and T. Shimanouchi, J. Chem. Phys. 47, 982 (1967).
[19]M. D. Sturge, Phys. Rev. B 8, 6 (1973).
[20]H. M. Gladney, Phys. Rev. 146, 253 (1966).
[21]W. A. Sibley, S. I. Yun, and W. E. Vehse, J. Phys. C 6, 1105 (1973).
[22]M. Ikeya and N. Itoh, J. Phys. Soc. Jpn. 26, 291 (1969).
[23]P. W. Anderson, Solid State Phys. 14, 147 (1963).
[24]J. Ferguson, H. J. Guggenheim, and Y. Tanabe, J. Appl. Phys. 36, 1046 (1965).
[25]J. Ferguson, E. R. Krausz, and H. J. Guggenheim, Mol. Phys. 27, 577 (1974).